The Journal of Experimental Biology 206, 3905-3911

doi:10.1242/jeb.00618

van der Waals and hygroscopic forces of adhesion generated by spider capture threads

Anya C. Hawthorn[1] and Brent D. Opell[2,*]

[1]*College of Veterinary Medicine* and [2]*Department of Biology, Virginia Tech, Blacksburg, VA 24061, USA*

*Author for correspondence (e-mail: bopell@vt.edu)

Accepted 21 July 2003

Summary

Cribellar thread is the most primitive type of sticky prey capture thread found in aerial spider webs. Its outer surface is formed of thousands of fine fibrils that issue from a cribellum spinning field. The fibrils of primitive cribellar thread are cylindrical, whereas those of derived threads have nodes. Cribellar threads snag on insect setae but also adhere to smooth surfaces. A previous study showed empirically that cylindrical fibrils use only van der Waals forces to stick to smooth surfaces, as their stickiness is the same under different humidity. By contrast, noded fibrils are stickier under high humidity, where they are presumed to adsorb atmospheric water and implement hygroscopic (capillary) adhesion. Here, we model thread stickiness according to these two adhesive mechanisms. These models equate stickiness with the force necessary to overcome the adhesion of fibril contact points in a narrow band along each edge of the contact surface and to initiate peeling of the thread from the surface. Modeled and measured thread stickiness values are similar, supporting the operation of the hypothesized adhesive forces and portraying an important transition in the evolution of spider threads. Cribellar threads initially relied only on van der Waals forces to stick to smooth surfaces. The appearance of fibril nodes introduced hydrophilic sites that implemented hygroscopic force and increased thread stickiness under intermediate and high humidity.

Key words: adhesion, capillary adhesion, cribellar thread, spider thread, *Hypochilus pococki*, *Hyptiotes cavatus.*

Introduction

Adhesion plays an important role in the locomotion and prey capture of many animals. It allows many insects (Eisner and Aneshansley, 2000; Federle et al., 2001; Gorb, 1998; Jiao et al., 2000; Lees and Hardie, 1988; Stork, 1980; Walker et al., 1985) and frogs (Emerson and Diehl, 1980; Gavin and Barnes, 1991; Green, 1981; Hanna and Barnes, 1991) and some reptiles (Autumn et al., 2000, 2002), mammals (Rosenberg and Rose, 1999) and spiders (Foelix, 1996) to cling to the surfaces on which they walk. It also plays a critical role in the prey capture of spiders. Most spiders that construct aerial capture webs incorporate sticky prey capture threads in their webs. These threads help retain insects that strike the web, giving a spider more time to locate, run to and subdue prey before they can escape from the web (Eberhard, 1989). The present study examines the adhesive mechanisms that cause cribellar thread, the most primitive type of prey capture thread spun by spiders (Coddington and Levi, 1991), to stick to smooth surfaces.

Cribellar thread is a composite thread formed of internal supporting fibers covered by a dense mat of several thousand small-diameter fibrils (Fig. 1; Hawthorn and Opell, 2002; Opell, 1994a, 1999; Peters, 1984, 1986). Cribellar threads are so named because these fibrils are spun from spigots of an abdominal spinning plate (sometimes divided) called the cribellum (Opell, 1994a, 1999; Peters, 1984). These protein fibrils are drawn from the cribellum by a setal comb on each of a spider's fourth legs (Eberhard, 1988; Opell, 2001; Opell et al., 2000) and formed around larger, internal supporting strands (Eberhard and Pereira, 1993) by adductions of the median spinnerets (Peters, 1986). The completed thread often forms a series of regular puffs (Opell, 1994a, 1999; Peters, 1984, 1986). Thread stickiness is determined by the number of fibrils that form its surface (Opell 1994a, 1999) and is modified by the dimensions of puffs and the manner in which a spider loops and folds a finished thread (Opell, 1995a, 2002).

The appearance of cribellar thread is associated with the appearance of aerial capture webs and corresponds to the origin of the Infraorder Araneomorphae, which contains 95% of all living spiders (Bond and Opell, 1998; Coddington and Levi, 1991). Some araneomorph spiders have lost the ability to produce cribellar threads as they have adopted other prey capture strategies and some have replaced cribellar thread with viscous thread (Coddington and Levi, 1991; Opell, 1997, 1998). Today, approximately 3606 species in 371 genera and 22 families spin cribellar threads (Griswold et al., 1999; Platnick, 2000). Of these, only 11 species in two genera of one family produce primitive, cylindrical, non-noded fibrils (Fig. 1B). The remainder produce fibrils with regularly spaced nodes (Fig. 1C; Hawthorn and Opell, 2002; Opell, 1994a). The only exceptions

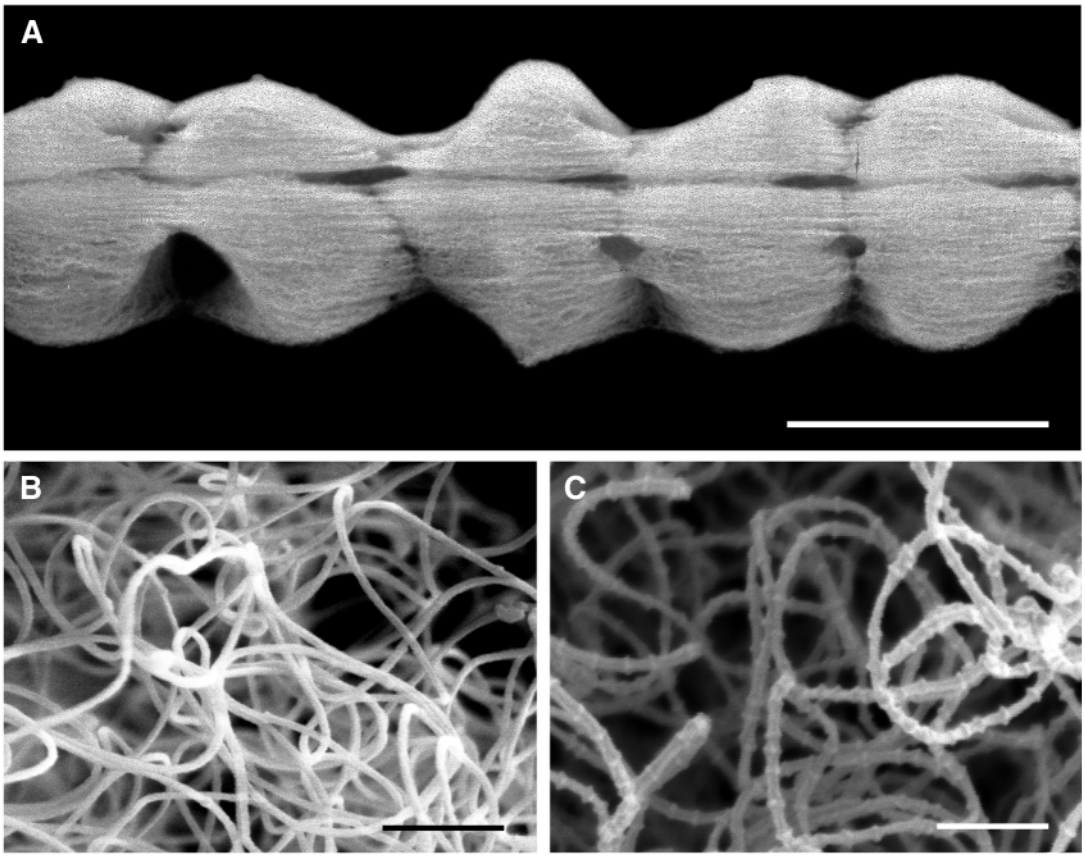

Fig. 1. (A) Cribellar thread of *Hyptiotes cavatus* (scale bar, 150 μm). (B) Cylindrical cribellar fibrils of *Hypochilus pococki* (scale bar, 400 nm). (C) Noded fibrils of *Hyptiotes cavatus* (scale bar, 200 nm).

are members of the family Filistatidae, which produce derived, flattened cribellar fibrils (Eberhard and Pereira, 1993).

Cribellar thread employs two stickiness mechanisms to hold a wide range of insect surfaces (Opell, 1994b): mechanical interlock (snagging) and adhesion. The fibrils on a thread's surface snag an insect's setae and hold them like the soft, looped side of a Velcro™ fastener (Opell, 1994b). However, cribellar thread also adheres to smooth surfaces such as graphite, polished steel, glass and beetle elytra (Eberhard, 1980; Opell, 1994b) by uncharacterized mechanisms. Adhesion to smooth surfaces can be achieved by van der Waals forces and electrostatic attraction (Allen, 1992a,b,c). Electrostatic attraction has been suggested for cribellar threads (Peters, 1984, 1986), but it has not been supported experimentally (Opell, 1995b).

van der Waals forces encompass two mechanisms: London dispersion forces and hygroscopic adhesion. The former depends only on the presence of nuclei and electrons and can operate between any two molecules that are in sufficiently close proximity (Hobsa and Zahradnik, 1988). These weak interactions arise when an instantaneous dipole in one molecule creates a synchronized instantaneous dipole in neighboring molecules. Surfaces can attract at a distance of 50 nm (Rigby et al., 1986). Hygroscopic adhesion, also known as capillary adhesion (Autumn et al., 2002; Stork, 1980), is generated when a thin film of water sticks to surfaces by adhesive forces and to other water molecules by cohesive forces, both of which involve hydrogen bonding. As the forces of adhesion are usually stronger than those of cohesion, the strength with which a water film holds surfaces together is determined by surface tension (Stork, 1980) and Laplace pressure (Israelachvili, 1992). It is not necessary for an organism to secrete this water, as hydrophilic substances can attract atmospheric moisture (Stork, 1980). For example, hydrophilic compounds in viscous capture threads attract atmospheric water to increase the volume of their droplets (Townley et al., 1991).

In a recent study (Hawthorn and Opell, 2002), we demonstrated that, when tested with a smooth surface, cribellar threads formed of non-noded fibrils registered the same stickiness under low and high humidity. By contrast, threads formed of noded fibrils registered greater stickiness under high humidity. These results support the hypothesis that plesiomorphic cribellar threads formed of non-noded fibrils employ only van der Waals forces of adhesion, whereas derived cribellar threads formed of noded fibrils implement hygroscopic adhesion. The present study uses an approach similar to that employed by Autumn et al. (2000, 2002) to provide an additional test of this hypothesis. Here, we model the forces of adhesion generated by van der Waals and hygroscopic forces for cribellar threads formed of noded and non-noded fibrils and compare these forces to the stickiness values measured for cribellar threads under high and low ambient humidity.

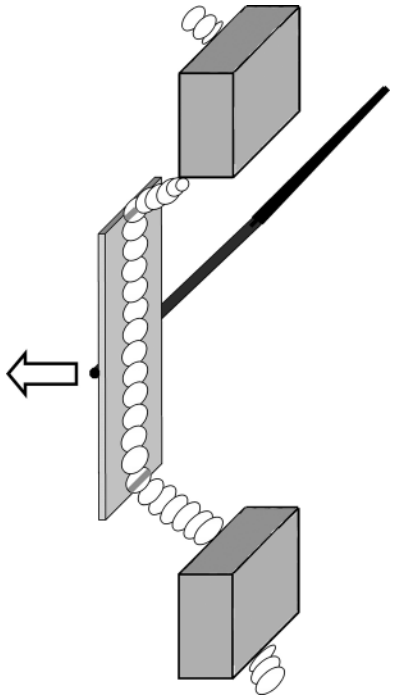

Fig. 2. Diagram of a contact plate that is attached to a needle and is being pulled from a cribellar thread held at either end by supports. Force is concentrated on bands of cribellar fibrils (hatched areas) at the two edges of the plate.

Previous studies of thread adhesion (e.g. Opell, 1994a,b, 1997, 1999) have reported stickiness as the μN of force required to pull each mm length of thread from a contact plate. These contact plates were made of fine sandpaper that yields the same stickiness values as plates made from a fleshfly wing (Opell, 1994c, 1997) and were 1960–2040 μm wide. This method was appropriate for the broad phylogenetic comparisons made in these studies. However, the models that we wish to develop require us to re-examine the way cribellar thread releases from a smooth surface. We believe that as a smooth contact plate pulls away from a thread, force is concentrated in a narrow band along each edge of the plate (Figs 2, 3). When this force overcomes the thread's adhesive forces, the thread peels rapidly from the edges of the plate towards its center, and the plate releases from the thread. To test this hypothesis, we measured the force required to overcome thread stickiness with narrow and wide contact plates. The hypothesis predicts that there should be little difference between the values registered by these plates.

Materials and methods

Collecting and measuring threads

We studied the non-noded threads of *Hypochilus pococki* Platnick 1987 (Hypochilidae) and noded threads of *Hyptiotes cavatus* (Hentz 1847) (Uloboridae). Threads of *H. pococki* were collected near the town of Roan Mountain, Craig Co., TN, USA and near Grandfather Mountain, Avery Co., NC, USA. The threads of *H. cavatus* were collected from the Virginia Tech campus and the forests of Montgomery and Giles Co., VA, USA. Threads spun by adult females were collected on microscope slides to which raised supports were glued at 4.8-mm intervals. Double-sided tape secured threads to the supports under their native tensions.

We measured the stickiness of some of these threads and photographed others under light and scanning electron (SEM) microscopes. Threads that were examined under the SEM were transferred to stubs and sputter coated with 4 nm of gold before being viewed at a magnification of approximately 100 000×. Low acceleration voltage of 2.00 kV prevented damage to the fibrils. Images of these fibrils and their included scale bars were saved digitally. Other threads were photographed under a dissecting microscope and a compound microscope equipped with differential interference contrast optics. These 35 mm slides were scanned to produce digital images. We measured these images of fibrils and threads with NIH Image and computed the number of point contacts between a thread and a smooth surface. We then used these data to model thread stickiness. Details of these procedures are described below.

Measuring thread stickiness

We measured thread stickiness with an instrument that incorporated a stainless steel strain gauge with a 2000 μm-wide contact plate (±40 μm) on its free end (Bond and Opell, 1998;

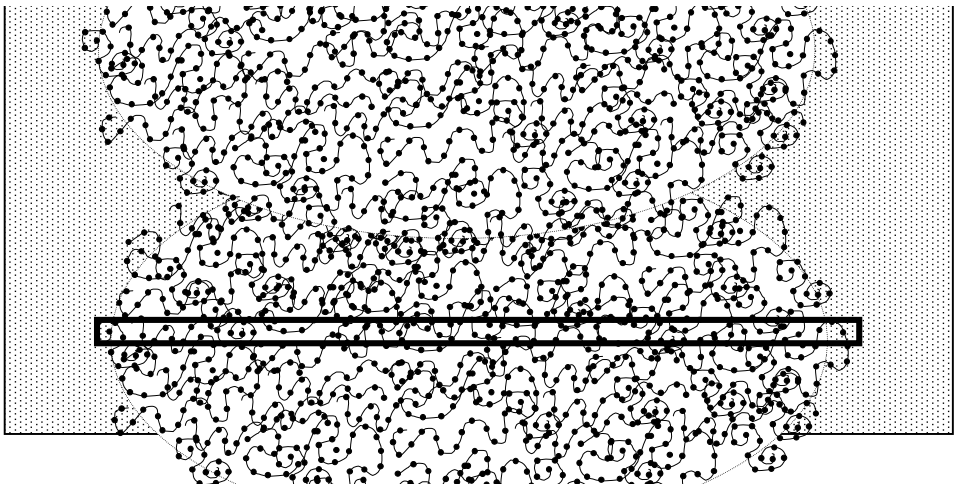

Fig. 3. Diagram of the band of contact (outlined by a dark rectangle) between a cribellar thread and the lower edge of the plate on the stickiness meter (Fig. 2), showing how the points of contact (closely spaced points on non-noded fibrils or the nodes of noded fibrils) were modeled.

Opell, 1994a,b, 1995a,b, 1997, 1998, 1999, 2002). A motorized advancement mechanism pressed the plate against a thread at a speed of 10.4 mm min^{-1} until a force of 19.61 μN was achieved. The thread was then withdrawn at 10.7 mm min^{-1} until it pulled free of the plate (Fig. 2). The needle's position on a scale at the time of release was recorded, and the mass required to deflect it to this position was multiplied by the accelerating force of gravity to yield the force (in Newtons) required to pull the plate from a thread. Under each humidity condition, we measured the stickiness of three threads per spider and used the mean value as the stickiness of this spider's thread at this humidity. Contact plates were surfaced with acetate from the non-sticky side of Scotch Magic™ Tape 810 (3M Co., St Paul, Minnesota, USA). This relatively nonpolar surface does not attract moisture, and SEM examination shows it to be fairly smooth even at the scale of tens of nanometers, at which the cribellar fibrils operate. Thus, we believe that there is maximum contact between cribellar fibrils and this surface. At a relative humidity (RH) of around 50%, noded cribellar thread sticks to this surface with a force comparable to that with which it holds fleshfly wings (Hawthorn and Opell, 2002). Thus, measured forces are in the range of those registered by a representative insect surface.

This stickiness instrument was enclosed in a clear, Plexiglas box. Low humidity (under 3% RH) was achieved by flushing the box with nitrogen. A small electric fan in the chamber ensured thorough mixing of the atmosphere. High humidity (near 100% RH) was achieved by bubbling the nitrogen through distilled water before it entered the box and by placing a piece of cloth dampened with distilled water over the fan. We measured the humidity and temperature with a digital hygrometer thermometer, dew point instrument (model 11-661-7B; Fisher Scientific, Pittsburgh, Pennsylvania, USA). These values were recorded at the beginning and end of each of the three stickiness measurements taken of a spider's thread and the mean values were used as the humidity and temperature for that trial.

Measuring stickiness with narrow and wide plates

Three narrow plates (1500, 1530 and 1560 μm widths) and three wide plates (2700, 2760 and 2760 μm widths) were prepared during the same one-hour period. Enough threads were collected from each of the webs produced by 13 adult female *H. cavatus* to permit four stickiness measurements with narrow and wide places, except in two cases where only three measurements were made with a plate of each width. Most threads were measured within 16 h of being produced and all within 36 h of being produced. After the stickiness of a series of threads from 2–4 webs was measured with a wide plate, the plate was removed from the needle and replaced with a new narrow plate. The narrow plate was then used to re-measure the first series of threads and then to take measurements of the next series of threads before being replaced by a new wide plate. In this fashion, stickiness measurements were alternated to control for the age of threads and contact plates. Narrow plates were used to measure stickiness under conditions (mean values: 23.1°C, 34.0% RH) similar to those used for wide plates (mean values: 23.3°C, 35.4% RH).

Modeling data and calculations

To model thread stickiness, we first determined the number of contact points (closely spaced points along non-noded cribellar fibrils and the nodes of noded cribellar fibrils) within the bands of contact (two areas, each the width of a flattened cribellar thread; Fig. 3) at the margins of contact plates. We then multiplied this total by the adhesive forces computed for a single contact point. The details of this process are described below.

The first step in modelling stickiness was to determine the number of nodes or contact points per thread area. For noded fibrils, we did this by determining the area of an SEM micrograph of cribellar thread, counting the number of nodes on the thread's surface fibrils (fibrils that were in sharp focus and not lying behind another fibril), and from these values computing node density. Thus, node density takes into account the coiled and stacked nature of the fibrils on the thread's surface. For *H. cavatus* threads, node density was 170±23 nodes μm^{-2} (N=5; all values are means ± S.D.).

We modeled the contact points of non-noded fibrils as a series of points separated by a distance of one fibril diameter. For *H. pococki*, the grand mean fibril diameter was 29±4.7 nm (N=6). The mean fibril diameter of each of these six individuals was calculated from the diameters of 10 fibrils from the cribellar thread. To determine the density of these contact points, we first measured the total length of the fibrils on a thread's surface that were in sharp focus and not overlain by other fibrils. We then divided this number by the total area of the micrograph to determine fibril density: 11 797±5222 nm μm^{-2} (N=6). Contact points are modeled as contiguous spheres whose diameters are equal to fibril diameter. Thus, the number of contact points along a fibril is equal to the fibril's length divided by its diameter. For *H. pococki*, this value is: 11 797 nm μm^{-2} divided by 29 nm = 407 contact points per μm^2.

The second modeling step involved determining the width of a thread when it was pressed against the stickiness meter's contact plate. We did this by placing a glass cover slip on a cribellar thread that was held on the supports of a microscope slide sampler (described above) and examining under a compound microscope the thread sectors that were suspended between the supports. For *H. cavatus* threads, which are formed of regularly spaced puffs (Fig. 1A), we measured maximum puff width, which had a mean value of 209.9±35.5 μm (N=8).

Hypochilus pococki threads have a less regular outline. Therefore, we photographed these threads under a compound microscope when they were pressed against a cover slip. We then measured the contact surface area of a known length of thread and divided this by the length to determine the mean contact width of the thread sample. The mean thread contact area was 168±68.2 μm^2 μm^{-1} (N=5) and the mean contact thread width was 168 μm.

In the third modeling step, we determined the areas of the two bands of contact between a cribellar thread and the upper and lower edges of a contact plate on the stickiness meter (Figs 2, 3). We computed the width of this band as the width of cribellar thread contacting a plate, and the length of the band as the diameter of one node or contact point plus the distance separating this point from an adjacent node or contact point. For *H. cavatus*, each band's width was the maximum width of a thread puff, and each band's length was a distance equal to one node diameter and one internode space (the distance between two adjacent fibril nodes) on either side of this node. We determined these values by first measuring 10 randomly selected nodes and internode spaces per thread, determining the mean per thread sample, and then computing the values of the grand means: node diameter = 35.3±1 nm (N=5), internode spacing = 85.5±7.2 nm (N=5). Thus, each band of contact had a width of 209.9 μm, a length of 0.121 μm and an area of 25.36 μm^2. For *H. pococki*, each band's width was equal to the mean thread width, and each band's length was equal to the diameter of a contiguous spherical contact point (= fibril diameter). Thus, each band had a width of 168 μm, a length of 0.029 μm and an area of 4.872 μm^2.

In the fourth modeling step, we determined the number of nodes or contact points in the contact bands of each species' threads. We did this by multiplying the area of contact by the node or contact point density. For *H. cavatus*, this value was: 25.36 μm^2 × 170 nodes μm^{-2} = 4311 nodes per band of contact. For *H. pococki*, this value was: 4.872 μm^2 × 407 contact points per μm^2 = 1983 contact points per band of contact.

In the fifth step, we modeled the van der Waals force (F_v) of a single point of contact as the force generated by the contact between a sphere and a plane, as described by the equation:

$$F = \frac{AR}{6D^2}, \quad (1)$$

where A is the Hamaker constant, taken to be 45×10^{-21} J (Autumn et al., 2002; Israelachvili, 1992), R is the radius of the sphere (for noded fibrils, the radius of a cribellar fibril node, and for cylindrical fibrils, the radius of a cribellar fibril) and D is the distance between the sphere and the substrate where van der Waals forces become significant (0.165 nm; Autumn et al., 2002; Israelachvili, 1992).

For *H. cavatus*, this computation was:

$$F_v = \frac{(45\times10^{-21})(17.5\times10^{-9})}{6(1.65\times10^{-10})^2} = 4.82\times10^{-9}\,\text{N} = 4.82\times10^{-3}\,\mu\text{N node}^{-1}. \quad (2)$$

For *H. pococki*, this computation was:

$$F_v = \frac{(45\times10^{-21})(14.5\times10^{-9})}{6(1.65\times10^{-10})^2} = 3.99\times10^{-9}\,\text{N} = 3.99\times10^{-3}\,\text{mN point}^{-1}. \quad (3)$$

In the sixth modeling step, we computed the hygroscopic adhesive force (F_H) created by a thin film of adsorbed water between a sphere and a plane using the equation:

$$F_H = 4\pi R\lambda_L\cos\theta, \quad (4)$$

where R is the radius of the sphere, λ_L is the surface energy of water (76 mJ m^{-2}) and θ is the angle of contact between the water and the substrate (Israelachvili, 1992), which was estimated to be 60° by observing a drop of water on the acetate surface used to measure thread stickiness. For *H. cavatus*, this computation was:

$$F_H = 4\pi R\lambda_L\cos\theta = 4\pi(17.7\times10^{-9})\times76\times0.5 = 8.36\times10^{-3}\,\mu\text{N node}^{-1}. \quad (5)$$

In the seventh step, we computed the total van der Waals forces exerted by both bands of contact. For *H. cavatus*, this computation is: 4.82×10^{-3} μN node^{-1} × 4311 nodes × 2 contact bands = 41.56 μN. For *H. pococki*, this computation was: 3.99×10^{-3} μN point^{-1} × 1983 points × 2 contact bands = 15.82 μN.

In the eighth step, we computed the total hygroscopic force exerted by both contact bands of *H. cavatus* threads: 8.36×10^{-3} μN node^{-1} × 4311 nodes × 2 contact bands = 72.08 μN.

In the ninth step, we computed the cumulative van der Waals and hygroscopic forces exerted by both contact bands of *H. cavatus* threads. This value is 41.56+72.08=113.64 μN.

Results

Stickiness measured with narrow and wide plates

Wide plates were, on average, 79% wider than narrow plates. However, the mean stickiness measured with wide plates (70.3±17.5 μN) was only 13% greater than that measured with narrow plates (62.3±19.5 μN). A paired t-test showed that the stickiness measured with wide and narrow plates did not differ (t=1.44, P=0.175, N=13). Additionally, when the force required to pull the contact plate free from a thread was divided by the length of the thread in contact with the plate (= plate width), narrow plates registered much greater values than wide plates (41.0 *vs* 25.7 μN mm^{-1} thread contact). Although the width of a contact plate may have a small effect on the stickiness measured, these results support the hypothesis that the force registered by the smooth surface is largely the force required to overcome the adhesion of narrow bands of cribellar fibrils along the outer edges of a contact plate (Figs 2, 3). Consequently, the assumptions made in our models of thread stickiness are supported.

Modeled and measured stickiness

Our simple mathematical models of van der Waals and hygroscopic forces yielded stickiness values that fall within one-half of a standard deviation of the measured values (Fig. 4). This agreement supports the hypothesized operation of van der Waals forces of adhesion in cribellar threads formed of non-noded fibrils and in threads formed of noded fibrils under very low humidity. It also supports the hypothesis that

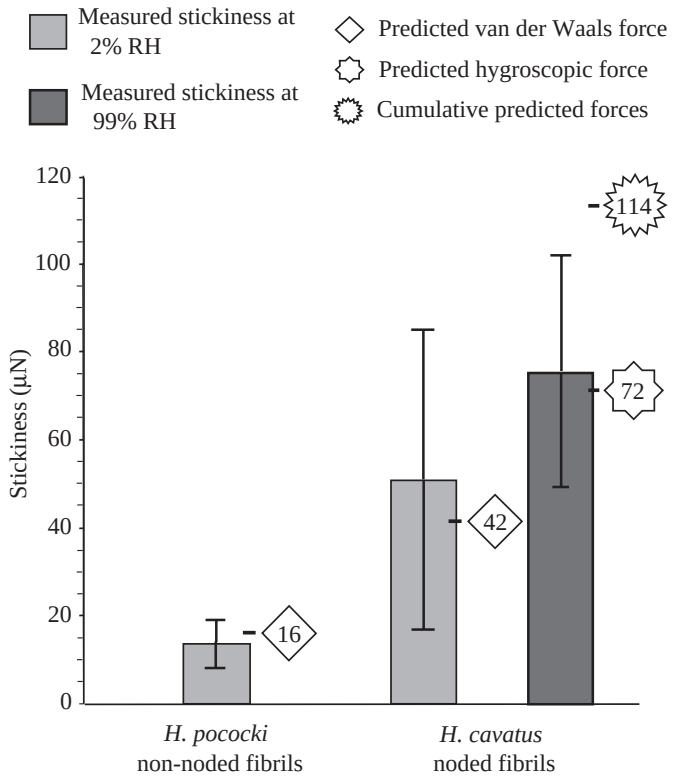

Fig. 4. Comparison of measured and modeled stickiness under high and low relative humidity (RH). Error bars of measured stickiness values represent ± 1 S.D.

at high humidity noded fibrils achieve greater stickiness by implementing hygroscopic forces of adhesion.

Hygroscopic forces alone are sufficient to explain the adhesion of cribellar threads formed of noded fibrils at high humidity. Under this condition, modeling adhesion as the combination of van der Waals and hygroscopic forces greatly overestimates thread stickiness. Consequently, it appears that both of these forces do not act simultaneously and that hygroscopic forces replace van der Waals forces at high ambient humidity.

Discussion

Derived cribellar prey capture thread formed of noded fibrils relies on three adhesive mechanisms to stick to a wide range of surfaces (Opell, 1994b): (1) its fibrils snag the setae and irregularities of insects, (2) under low humidity its fibrils cling to smooth surfaces by van der Waals forces and (3) under high humidity its fibrils cling to smooth surfaces by hygroscopic forces. Evidence that this hygroscopic force also operates at low ambient humidity comes from measurements taken to compare stickiness measured with contact plates of different widths. The mean width of the six contact plates used in these measurements of *H. cavatus* threads was 2135 μm, and the mean RH at which these measurements were taken was 35%. The resulting mean stickiness of 66 μN was 88% of that registered at an RH of 99% by 2000 μm-wide contact plates. Thus, hygroscopic force probably operates to some extent under most natural environmental conditions.

Primitive cribellar threads formed of cylindrical fibrils rely only on van der Waals forces to stick to smooth surfaces (Hawthorn and Opell, 2002). Consequently, an increase in the stickiness of cribellar threads formed of these fibrils requires an increase in the number of fibrils that contact a surface. This can be achieved by increasing the number of spigots on the cribellum (Opell, 1994a, 1999) or by configuring cribellar threads so that more fibrils contact the surface (Opell, 2002). Either strategy requires an increase in protein expenditure. The appearance of noded cribellar fibrils was probably favored because it increased thread adhesion at most ambient humidity conditions without requiring a proportional increase in protein expenditure. As noded fibrils press against a smooth surface, it appears that the nodes are the principal points of contact. Thus, nodes seem to reduce the area of contact between fibrils and surfaces. This further emphasizes the strength of adhesive forces that operate at the nodes. It is presumably here that the hydrophilic regions of the silk reside.

Our models not only document the ability of cribellar threads to implement van der Waals and hygroscopic forces but they also provide insights into the operation and design of these threads. The peeling phenomenon on which our models are based probably operates to some degree even on insect surfaces that are covered by setae. Thus, the prominent cribellar thread puffs that characterize capture threads spun by members of the orb-weaving family Uloboridae (Opell, 1994a,b, 1999) may have been selected to maximize thread efficiency. If thread stickiness is, to a large extent, a measure of the threshold force necessary to overcome bands of adhesion along the edges of a contact surface, then producing threads that are puffed rather than of uniform width would represent an optimal expenditure of material. Thread puffs maximize the widths of contact with the edges of a surface and, consequently, the forces of adhesion generated in these areas. Narrower thread regions between these edge areas of contact probably do not greatly reduce thread stickiness, as these intermediate regions only experience force after the peeling threshold of edge areas has been exceeded.

The nodes of derived cribellar fibrils may contribute to thread function in additional ways. Nodes may make it more difficult for fibrils to slide over one another when cribellar threads are being spun and after they have been incorporated into webs. This would reduce the tendency for fibrils to pack together and, thereby, allow more fibrils to contact a prey when it strikes the web. Noded fibrils may also help absorb the force that is generated when an insect strikes the web and as it struggles to free itself. They could do so by offering more resistance than cylindrical fibrils to forces that cause fibrils to slide over one another and to pull free from the larger supporting fibers inside the thread. This resistance to sliding might also cause the internode segments of fibrils to stretch and, thereby, dissipate additional energy. A complete understanding of the functional properties of cribellar threads

awaits the characterization of the molecular architecture and functional properties of their fibrils, such as is beginning to be done for other types of spider silks (Gosline et al., 1999; Guerette et al., 1996; Hayashi and Lewis, 1998, 2000; Hinman and Lewis, 1992).

Jill Sible and Francis Webster offered helpful suggestions during the development and execution of this study. Funding was provided by the American Arachnological Society, the National Science Foundation (grant IBN-9417803) and Virginia Tech's Department of Biology and Graduate Research and Development Program.

References

Allen, K. W. (1992a). Theories of adhesion. In *Handbook of Adhesion* (ed. D. E. Packham), pp. 473-475. Essex, UK: Longman Scientific and Technical.

Allen, K. W. (1992b). Mechanical theory. In *Handbook of Adhesion* (ed. D. E. Packham), pp. 273-275. Essex, UK: Longman Scientific and Technical.

Allen, K. W. (1992c). Adsorption theory of adhesion. In *Handbook of Adhesion* (ed. D. E. Packham), pp. 39-41. Essex, UK: Longman Scientific and Technical.

Autumn, K., Liang, Y. A., Hsieh, S. T., Zesch, W., Chan, W. P., Kenny, T. W., Fearing, R. and Full, R. J. (2000). Adhesive force of a single gecko foot-hair. *Nature* **405**, 681-684.

Autumn, K., Sitti, M., Liang, Y. A., Peattie, A. M., Hansen, W. R., Sponberg, S., Kenny, T. W., Fearing, R., Israelachvili, J. and Full, R. J. (2002). Evidence for van der Waals adhesion in gecko setae. *Proc. Natl. Acad. Sci. USA* **99**, 12252-12256.

Bond, J. E. and Opell, B. D. (1998). Testing adaptive radiation and key innovation hypothesis in spiders. *Evolution* **52**, 403-414.

Coddington, J. A. and Levi, H. W. (1991). Systematics and evolution of spiders (Araneae). *Annu. Rev. Ecol. Syst.* **22**, 565-592.

Eberhard, W. G. (1980). Persistent stickiness of cribellar silk. *J. Arachnol.* **8**, 283.

Eberhard, W. G. (1988). Combing and sticky silk attachment behavior by cribellate spiders and its taxonomic implications. *Bull. Br. Arachnol. Soc.* **7**, 247-251.

Eberhard, W. G. (1989). Effects of orb web orientation and spider size on prey retention. *Bull. Br. Arachnol. Soc.* **8**, 45-48.

Eberhard, W. G. and Pereira, F. (1993). Ultrastructure of cribellate silk of nine species in eight families and possible taxonomic implications. (Araneae: Amaurobiidae, Deinopidae, Desidae, Dictynidae, Filistatidae, Hypochilidae, Stiphidiidae, Tengellidae). *J. Arachnol.* **21**, 161-174.

Eisner, T. and Aneshansley, D. J. (2000). Defense by foot adhesion in a beetle (*Hemisphaerota cyanea*). *Proc. Natl. Acad. Sci. USA* **97**, 6568-6573.

Emerson, S. B. and Diehl, D. (1980). Toe pad morphology and mechanisms of sticking in frogs. *Biol. J. Linn. Soc.* **13**, 199-216.

Federle, W., Brainerd, E. L., McMahon, T. A. and Hölldobler, B. (2001). Biomechanics of the movable pretarsal adhesive organ in ants and bees. *Proc. Natl. Acad. Sci. USA* **98**, 6215-6220.

Foelix, R. F. (1996). *Biology of Spiders.* 2nd edition. New York: Oxford University Press.

Gavin, H. and Barnes, W. J. P. (1991). Adhesion and detachment of the toe pads of tree frogs *J. Exp. Biol.* **155**, 103-125.

Gorb, S. N. (1998). The design of the fly adhesive pad: distal tenent setae are adapted for the delivery of an adhesive secretion. *Proc. R. Soc. Lond. B* **265**, 747-752.

Gosline, J. M., Cuerette, P. A., Ortlepp, C. S. and Savage, K. N. (1999). The mechanical design of spider silks: from fibroin sequence to mechanical function. *J. Exp. Biol.* **202**, 3295-3303.

Green, D. M. (1981). Adhesion and the toe pads of tree frogs. *Copeia* **4**, 790-796.

Griswold, C. E., Coddington, J. A., Platnick, N. I. and Forster, R. R. (1999). Towards a phylogeny of entelegyne spiders (Araneae, Araneomorphae, Entelegynae). *J. Arachnol.* **27**, 53-63.

Guerette, P. A., Ginzinger, D. G., Weber, B. H. F. and Gosline, J. M. (1996). Silk properties determined by gland-specific expression of a spider fibroin gene family. *Science* **272**, 112-114.

Hanna, G. and Barnes, W. J. P. (1991). Adhesion and detachment of the toe pads of tree frogs. *J. Exp. Biol.* **155**, 103-125.

Hawthorn, A. C. and Opell, B. D. (2002). Evolution of adhesive mechanisms in cribellar spider capture thread: evidence for van der Waals and hygroscopic forces. *Biol. J. Linn. Soc.* **77**, 1-8.

Hayashi, C. and Lewis, R. V. (1998). Evidence from flagelliform silk cDNA for the structural basis of elasticity and modular nature of spider silks. *J. Mol. Biol.* **275**, 773-778.

Hayashi, C. and Lewis, R. V. (2000). Molecular architecture and the evolution of a modular spider silk protein gene. *Science* **287**, 1477-1479.

Hinman, M. B. and Lewis, R. V. (1992). Isolation of a clone encoding a second dragline silk fibronin. *J. Biol. Chem.* **26**, 19320-19324.

Hobsa, P. and Zahradnik, R. (1988). *Intermolecular Complexes: The Role Of Van Der Waals Systems In Physical Chemistry And In The Biodisciplines.* New York: Elsevier Science.

Israelachvili, J. N. (1992). *Intermolecular And Surface Forces.* Santa Barbara, CA: Academic Press.

Jiao, Y., Gorb, S. and Scherge, M. (2000). Adhesion measured on the attachment pads of *Tettigonia viridissima* (Orthroptera, Insecta). *J. Exp. Biol.* **203**, 1887-1895.

Lees, A. D. and Hardie, J. (1988). The organs of adhesion in the aphid *Megoura viciae*. *J. Exp. Biol.* **136**, 209-228.

Opell, B. D. (1994a). Factors governing the stickiness of cribellar prey capture threads in the spider family Uloboridae. *J. Morph.* **221**, 111-119.

Opell, B. D. (1994b). The ability of spider cribellar prey capture thread to hold insects with different surface features. *Funct. Ecol.* **8**, 145-150.

Opell, B. D. (1994c). Increased stickiness of prey capture threads accompanying web reduction in the spider family Uloboridae. *Funct. Ecol.* **8**, 85-90.

Opell, B. D. (1995a). Ontogenetic changes in cribellum spigot number and cribellar prey capture thread stickiness in the spider family Uloboridae. *J. Morph.* **224**, 47-56.

Opell, B. D. (1995b). Do static electric forces contribute to the stickiness of a spider's cribellar prey capture threads? *J. Exp. Zool.* **273**, 186-189.

Opell, B. D. (1997). The material cost and stickiness of capture threads and the evolution of orb-weaving spiders. *Biol. J. Linn. Soc.* **62**, 443-458.

Opell, B. D. (1998). Economics of spider orb-webs: the benefits of producing adhesive capture thread and recycling silk. *Funct. Ecol.* **12**, 613-624.

Opell, B. D. (1999). Changes in spinning anatomy and thread stickiness associated with the origin of orb-weaving spiders. *Biol. J. Linn. Soc.* **68**, 593-612.

Opell, B. D. (2001). Cribellum and calamistrum ontogeny in the spider family Uloboridae: linking functionally related but separate silk spinning features. *J. Arachnol.* **29**, 220-226.

Opell, B. D. (2002). How spider anatomy and thread configuration shape the stickiness of cribellar prey capture threads. *J. Arachnol.* **30**, 10-19.

Opell, B. D., Sandidge, J. S. and Bond, J. E. (2000). Exploring functional associations between spider cribella and calamistra. *J. Arachnol.* **28**, 43-48.

Peters, H. M. (1984). The spinning apparatus of Uloboridae in relation to the structure and construction of capture threads (Arachnida, Araneida). *Zoomorph.* **104**, 96-104.

Peters, H. M. (1986). Fine structure and function of capture threads. In *Ecophysiology of Spiders* (ed. W. Nentwig), pp. 187-202. New York: Springer Verlag.

Platnick, N. I. (2000). Estimating spider numbers. *Am. Arachnol.* **61**, 8-9.

Rigby, M., Smith, E. B., Wakeham, W. A. and Maitland, G. C. (1986). *The Forces Between Molecules*. New York: Oxford University Press.

Rosenberg, H. I. and Rose, R. (1999). Volar adhesive pads of the feathertail glider, *Acrobates pygmaeus* (Marsupialia; Acrobatidae). *Can. J. Zool.* **77**, 233-248.

Stork, N. E. (1980). Experimental analysis of adhesion of *Chrysolina polita* (Chrysomelidae, Coleoptera) on a variety of surfaces. *J. Exp. Biol.* **88**, 91-107.

Townley, M. A., Bernstein, D. T., Gallenger, K. S. and Tillinghast, E. K. (1991). Comparative study of orb web hygroscopicity and adhesive spiral composition in three araneid spiders. *J. Exp. Zool.* **259**, 154-165.

Walker, G., Yule, A. B. and Ratcliffe, J. (1985). The adhesive organ of the blowfly *Calliphora vomitorix*: a functional approach (Diptera, Calliphoridae). *J. Zool.* **205**, 297-307.